第 40 卷 第 3 期
2025 年 6 月

新型炭材料（中英文）
New Carbon Materials

Cite this: New Carbon Materials, 2025, 40(3): 518-538

Read Online

Review

A review of graphene assembled films as platforms for electrochemical reactions

ZHU Yong-fang[1,2,†], JI Xiao-dong[1,2,†], PAN Wen-kai[1,2], WU Geng[1], LI Peng[3], LIU Bo[1,3,*], HE Da-ping[1,2,3,*]

(1. *Sanya Science and Education Innovation Park of Wuhan University of Technology*, *Sanya* 572000, *China*;
2. *School of Materials Science and Engineering*, *Wuhan University of Technology*, *Wuhan* 430070, *China*;
3. *School of Physics and Mechanics*, *Hubei Engineering Research Center of RF-Microwave Technology and Application*, *Wuhan University of Technology*, *Wuhan* 430070, *China*)

Abstract: Because of their low electrical conductivity, sluggish ion diffusion, and poor stability, conventional electrode materials are not able to meet the growing demands of energy storage and portable devices. Graphene assembled films (GAFs) formed from graphene nanosheets have an ultrahigh conductivity, a unique 2D network structure, and exceptional mechanical strength, which give them the potential to solve these problems. However, a systematic understanding of GAFs as an advanced electrode material is lacking. This review focuses on the use of GAFs in electrochemistry, providing a comprehensive analysis of their synthesis methods, surface/structural characteristics, and physical properties, and thus understand their structure-property relationships. Their advantages in batteries, supercapacitors, and electrochemical sensors are systematically evaluated, with an emphasis on their excellent electrical conductivity, ion transport kinetics, and interfacial stability. The existing problems in these devices, such as chemical inertness and mechanical brittleness, are discussed and potential solutions are proposed, including defect engineering and hybrid structures. This review should deepen our mechanistic understanding of the use of GAFs in electrochemical systems and provide actionable strategies for developing stable, high-performance electrode materials.

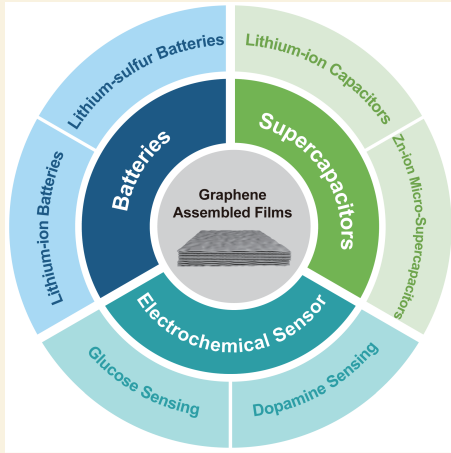

Key words: Graphene assembled films; Batteries; Supercapacitors; Electrochemical sensors; Synthesis methods

1 Introduction

Amidst rapid advancements in transportation, information technology, and healthcare sectors, the surging demand for energy storage and portable devices has imposed unprecedented challenges on electrochemical technologies. At present, batteries and capacitors dominate in energy storage systems, but their limited energy density and cycle life still could not meet the existing needs. Therefore, new materials need to be developed to improve their performance. Concurrently, the slow detection speed and poor reproducibility of current electrochemical sensors critically restrict their applications in sensing. Traditional metals and their alloys have been widely employed in electrochemical energy storage and sensing[1–9]. However, their complex fabrication processes, susceptibility to corrosion, high mass density, poor flexibility, and reliance on non-renewable resources pose critical constraints on technological innovation[10–18].

Carbon-based electrode materials, as a core material system in electrochemical energy storage, have emerged as a frontier research hotspot due to their unique physicochemical properties[19–24]. Compared to traditional metal or metal oxide electrodes, carbon materials exhibit multidimensional advantages: (1)

Received: March 01, 2025
Revised: May 13, 2025
Accepted: May 14, 2025
DOI: 10.1016/S1872-5805(25)60992-9
CSTR: 32158.14.S1872-5805(25)60992-9

Their abundant raw material sources and mature synthesis processes significantly reduce economic barriers for large-scale applications. (2) Their exceptional chemical inertness within a wide voltage window effectively suppresses side reactions such as electrolyte decomposition. (3) Their biocompatibility expands application potential in specialized scenarios like implantable medical devices. Structurally, carbon materials form diverse configurations, including graphene, carbon nanotubes, and porous carbons, through flexible combinations of sp^2/sp^3 hybridized bonds. This structural tunability enables precise regulation of surface electronic states, pore topology, and defect concentrations, exemplified by nitrogen-sulfur co-doping achieving active site densities up to 10^{20} cm^{-3}. By integrating superior electron transport properties with optimized ion diffusion pathways, carbon-based materials fulfill multifunctional roles in energy storage systems: as active material carriers, their high specific surface area enhances charge storage density; as conductive additives, they form a 3D interconnected network, which not only enhances electron transport in silicon-based anodes but also mechanically confines volume expansion, thereby leading to significant enhancement in electrochemical reaction kinetics and prolonged cycle life. In addition, as coating layers, it can isolate the direct contact between the active material and the electrolyte, then inhibit side reactions (such as electrolyte decomposition and excessive growth of the SEI film), thus improve the capacity retention[25–29]. This multifunctional integration renders them indispensable in lithium-ion batteries, supercapacitors, and metal-air battery systems[30–33].

Graphene assembled films (GAFs), as representative novel carbon materials, exhibit exceptional promise in electrochemical energy storage and sensing applications due to their superior conductivity, high specific surface area, and architecturally tunable two-dimensional network structures[34–35]. The unique electronic structure of graphene, featuring delocalized π bonds from sp^2 hybridized orbitals, and its topological characteristics (maintaining a C—C bond length of 0.142 nm even at single atomic layer thickness) endows it with intrinsic conductivity up to 10^6 S m^{-1} and a theoretical specific surface area of 2630 m^2 g^{-1}, making it an ideal platform for constructing high efficiency electrochemical interfaces. Since its discovery in 2004, graphene nanomaterials have been extensively studied as surface modification layers[36–39]. However, limitations such as structural instability, electrochemical degradation, and aggregation issues have hindered their practical applications[40]. To address these challenges, researchers have developed strategies like vacuum-assisted self-assembly, wet-spinning, and electrostatic repulsion to achieve the macro-scale transformation of graphene.

Here, we comprehensively delineated the applications and advantages of GAFs in electrochemical systems, highlighting their transformative impact on energy and sensor technologies. We first elaborated on fabrication methodologies for GAFs, including evaporation-induced layer-by-layer self-assembly, spray coating, spin coating, high-temperature thermal reduction, chemical vapor deposition, wet-spinning, and vacuum filtration, with a critical analysis of their respective merits and limitations. A focused investigation is conducted on the microstructural morphology and physical properties of self-assembled graphene films prepared by high-temperature thermal reduction, accompanied by comparative assessments of their electrical conductivity. Subsequently, we systematically reviewed advancements in graphene assembled film applications across batteries, supercapacitors, and electrochemical sensors (Fig. 1), emphasizing performance enhancements in charge storage density, ion diffusion kinetics, and sensing sensitivity. The discussion concludes with an outlook on future research trajectories, addressing challenges in scalable production, defect engineering, and multifunctional integration for next-generation electrochemical devices.

2 Preparation methods of graphene assembled films

The primary methods for fabricating graphene assembled films encompass evaporation-induced layer-by-layer self-assembly[27–29], spray coating[41–43],

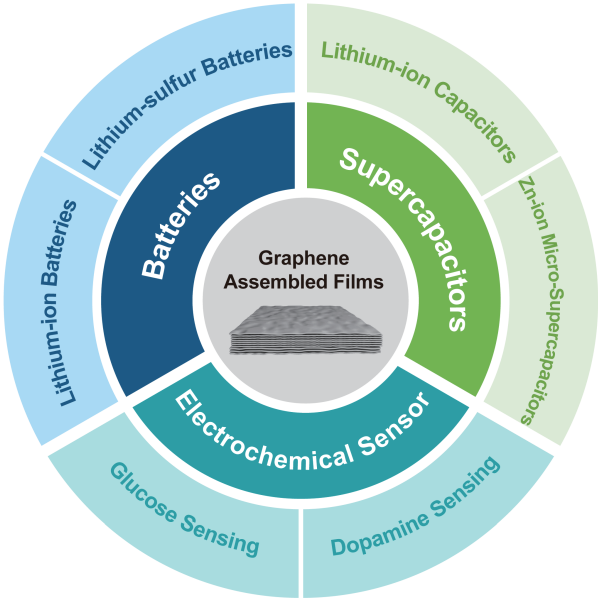

Fig. 1 Applications of graphene assembled films in electrochemistry

spin coating[33–34], high-temperature thermal reduction[35–36], chemical vapor deposition[40], wet-spinning[31] and vacuum filtration[32]. These processes exhibit pronounced disparities in film-forming mechanisms, structural modulation and performance optimization[33].

2.1 Layer by layer self-assembly methods

Layer-by-layer self-assembly constructs thin films through alternate stacking of oppositely charged materials, offering precise thickness control and highly ordered multiscale architectures for complex surfaces or multifunctional composite films[27–29]. Layer-by-layer self-assembly, as a classical physical assembly strategy (Fig. 2a)[37], it operates on the dynamic equilibrium between solvent evaporation-induced capillary forces and intermolecular interactions (e.g., van der Waals forces, π-π stacking) among graphene nanosheets, enabling progressive and ordered nanolayer stacking[47]. The standard protocol involves casting graphene-based slurries into polytetrafluoroethylene (PTFE) molds or onto substrates, followed by solvent evaporation under ambient or controlled temperatures to obtain freestanding films. This method demonstrates significant industrial potential due to equipment simplicity (eliminating high-temperature furnaces or vacuum systems), scalability from laboratory to manufacturing settings, and high material utilization efficiency, particularly advantageous for low-cost precursors like graphene oxide (GO). Technologically, it has evolved from early static equilibrium assembly to electric/magnetic field-assisted dynamic alignment and surfactant-mediated interlayer modifications, which markedly improve layer packing density and orientation uniformity. Nevertheless, the layer-by-layer deposition mechanism limits throughput for thick-film fabrication, while stringent control of process parameters (solvent evaporation rate, temperature/humidity) increases operational complexity. The inherent mechanical weakness from weak interlayer interactions remains a critical barrier for structural material applications[49].

2.2 Spray coating methods

Spray coating is a technique that forms uniform thin films by atomizing liquid material into fine droplets and spraying them onto a substrate surface.[41–43]. The spray coating method involves depositing the GO dispersion onto preheated substrates (Fig. 2b)[44], where microdroplet evaporation minimizes solute loss to <5%. Technological breakthroughs include: evolution from primitive concentration control to multiparameter synergy (concentration/layer number/evaporation time) achieving tunable film density[45]. Ultrasonic atomization refining droplet size from micron-scale to submicron-level, significantly improving coating uniformity. Compared to vacuum filtration or spin coating, spray coating combines equipment simplicity and multi-substrate compatibility (glass/metal/polymers), enabling meter-scale continuous production of GO films[46]. Nevertheless, the "coffee-ring" effect during high-speed spraying still limits thickness uniformity to ±15%, requiring gradient surface-tension dispersants for compensation.

2.3 Spin coating methods

Spin coating uses centrifugal force from a high-speed rotating substrate to spread solutions into uniform films, ideal for ultrathin coatings with consistent thickness but with low material efficiency[48]. Spin coating involves depositing a GO dispersion onto a heated substrate (Fig. 2c)[50], synergistic optimization of substrate temperature, rotational speed, coating cycles, and duration reduces GO nanosheet lateral mo-

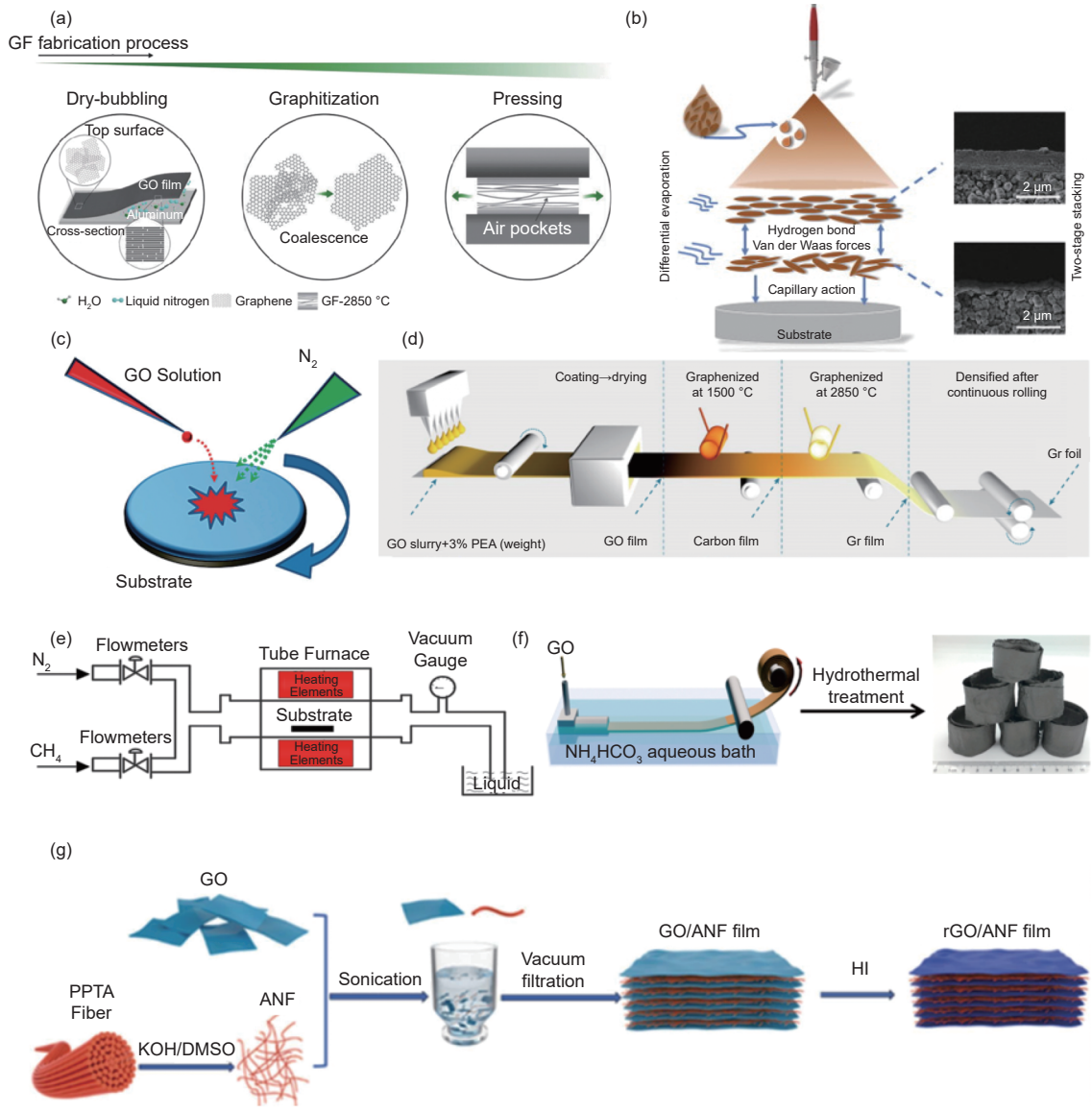

Fig. 2 Preparation methods of graphene assembled films. (a) Layer-by-layer self-assembly (Reprinted with permission, Copyright 2021, MDPI)[37]. (b) Spray coating (Reprinted with permission, Copyright 2017, Elsevier)[44]. (c) Spin coating (Reprinted with permission, Copyright 2008, American Chemical Society)[50]. (d) High-temperature thermal reduction (Reprinted with permission, Copyright 2024, Springer Nature)[78]. (e) Chemical vapor deposition (Reprinted with permission, Copyright 2019, Springer Nature)[61]. (f) Wet-spinning (Reprinted with permission, Copyright 2019, Elsevier)[67]. (g) Vacuum filtration (Reprinted with permission, Copyright 2024, Elsevier)[72]

bility by 80%, forming highly interlocked homogeneous architectures[33]. Evolution from single-step to multi-cycle intermittent coating, coupled with immersion capillary forces and like-charge repulsion, decreases interlayer water content from 12% to 2%, compressing interlayer spacing from ~ 0.8 to 0.36 nm. Nevertheless, compared to vacuum filtration, its process complexity increases operational costs by 40%, while edge thickness variation reaches ±10% in large-area coatings, necessitating rotational acceleration gradient control for uniformity improvement[51].

2.4 High-temperature thermal reduction methods

Films can be prepared by high-temperature thermal reduction methods using reducing precursors in inert atmospheres, enabling high-conductivity or functional materials but requiring specialized high-temperature equipment[52]. The high-temperature thermal reduction method begins with a GO slurry (Fig. 2d)[78], followed by gradient heating removing >90% interlayer oxygen-containing groups, and graphitization compressing grain boundaries from micron-scale to submicron-level[53–56]. Final rolling

achieves film thickness uniformity of ±1.2 μm with in-plane conductivity increased by 4 orders of magnitude. However, the process suffers from high energy consumptionand transverse crack density in thick films, requiring low-temperature catalytic graphitization to balance performance and cost[57–58].

2.5 Chemical vapor deposition methods

Dense and high-purity films can be produced by Chemical vapor deposition (CVD) using gas-phase precursor reactions, excelling in fabricating millimeter-sized single-crystal graphene with ultralow grain boundary density and exceptional carrier mobility, making them ideal for high-end electronics[59–60]. CVD is performed under nitrogen protection (Fig. 2e)[61]. It employs nitrogen protection: cemented carbide substrates are ultrasonically cleaned in acetone and placed in a quartz reactor, where high-purity nitrogen purging establishes a low-oxygen environment[62]. Technological breakthroughs include three aspects: a three-stage temperature program tripling methane pyrolysis efficiency; ethanol/methane mixed gas sources increasing monolayer growth rate from 1 to 10 μm min^{-1}; and dual-temperature-zone reactors (high-T growth/low-T crystallization) enabling millimeter-scale grains. Closed-loop pressure control coupled with exhaust treatment reduces film defect density by 80%[63]. Nevertheless, the requirement for precise control of many parameters (temperature/pressure/flow rate) results in high complexity and energy consumption[64].

2.6 Wet spinning methods

Wet spinning solidifies polymer solutions into films/fibers by coagulation baths, offering continuous production capability and tunable hierarchical porosity, delivering macroscopic assemblies with mechanical strength >200 MPa for flexible devices and porous films[65–66]. Technological breakthroughs originate from lyotropic liquid crystal (LC) phase engineering: LC phases formed by amphiphilic molecules in polar solvents (Fig. 2f)[67], induced isotropic-to-nematic phase transitions in GO dispersions at critical concentrations, significantly enhancing nanosheet alignment[68–70]. Compared to aggregation-prone pristine graphene, GO forms stable LC phases in aqueous media due to abundant hydrophilic groups. High-shear flow fields coupled with rapid solvent exchange effectively reduce interlayer hydration, enabling long-range ordered architectures. Reduced GO (rGO) films exhibit exceptional in-plane conductivity with markedly improved ion transport efficiency over conventional methods. Nevertheless, topological defects generated during thermal reduction cause substantial conductivity degradation, necessitating novel in situ remediation strategies for performance optimization[71].

2.7 Vacuum filtration methods

The vacuum filtration method stands as a cornerstone technique for graphene film fabrication, with its fundamental advantage lying in pressure gradient-driven nanosheet alignment for thickness-controlled uniform films. Technological progression is evidenced by innovations from single-component systems to multifunctional heterostructures. Ren et al. demonstrated enhanced mechanical integrity while preserving conductivity through aramid nanofiber/rGO composites (Fig. 2g)[72]. Zhang et al. engineered ion-selective channels by amine-confined interlayer spaces to optimize film separation[73]. Additional studies improved energy storage cyclability through phase-change material/graphene aerogel hybrid[74]. Nevertheless, the method's efficiency remains thickness-dependent, with limited precursor compatibility, requiring integration with advanced phase separation strategies for material diversity expansion.

3 Morphology and characterization of GAFs

The following discussion addresses the microstructural and physical property characteristics of the graphene film. Initial characterization of the film's surface and cross-section (Fig. 3a) reveals abundant micro-wrinkles, which enhance the effective surface area to optimize electrode-electrolyte interfacial reactivity[75]. Cross-sectional analysis (Fig. 3b) confirms a tightly stacked, ordered multilayered architecture[76]. Macroscopically, large-depth 3D microscopy (Fig. 3c)

demonstrates a uniformly flat surface morphology. Transmission electron microscopy (TEM) of pristine graphene nanosheets (Fig. 3d) highlights their intrinsic wrinkled configuration, which underpins the film's mechanical flexibility. High-resolution TEM (Fig. 3e) resolves defect-free lattice fringes, confirming the structural coherence of graphene as the primary constituent[77]. The measured lattice spacing of 0.34 nm (Fig. 3f) aligns with the (002) diffraction peak at 26.5° in XRD analysis (Fig. 3g), corresponding to an interlayer spacing of ~ 0.336 nm. The XRD patterns of GAF with different grain sizes vary, mainly reflected in the size of the (002) diffraction peak half width, which is proportional to each other. The change in peak position of the (002) diffraction peak is mainly influenced by the degree of graphitization of the GAF. The higher the degree of graphitization, the stronger the interlayer interaction of graphene, and the corresponding interlayer spacing is smaller, resulting in a shift of the (002) reflection peak towards larger angles. In addition, the type of precursor, number of functional groups, temperature, etc. during the synthesis process may also have potential effects on the diffraction peaks. Raman specturm (Fig. 3h) exhibits a weak *D* band (defect-related) and a prominent *G*-band (sp^2 hybridization), indicative of high graphitic crystallinity, further corroborated by the intense 2*D* band at 2714 cm^{-1}. The different degrees of defects in GAF correspond to different Raman spectra, mainly reflected in the proportional relationship between the *D* peak and the *G* peak. XPS spectrum (Fig. 3i) confirm near-complete removal of oxygen-containing functional groups post high-temperature thermal reduction. In addition, the number of oxygen-containing functional groups on the surface of GAFs varies with the degree of reduction, which is reflected in the different

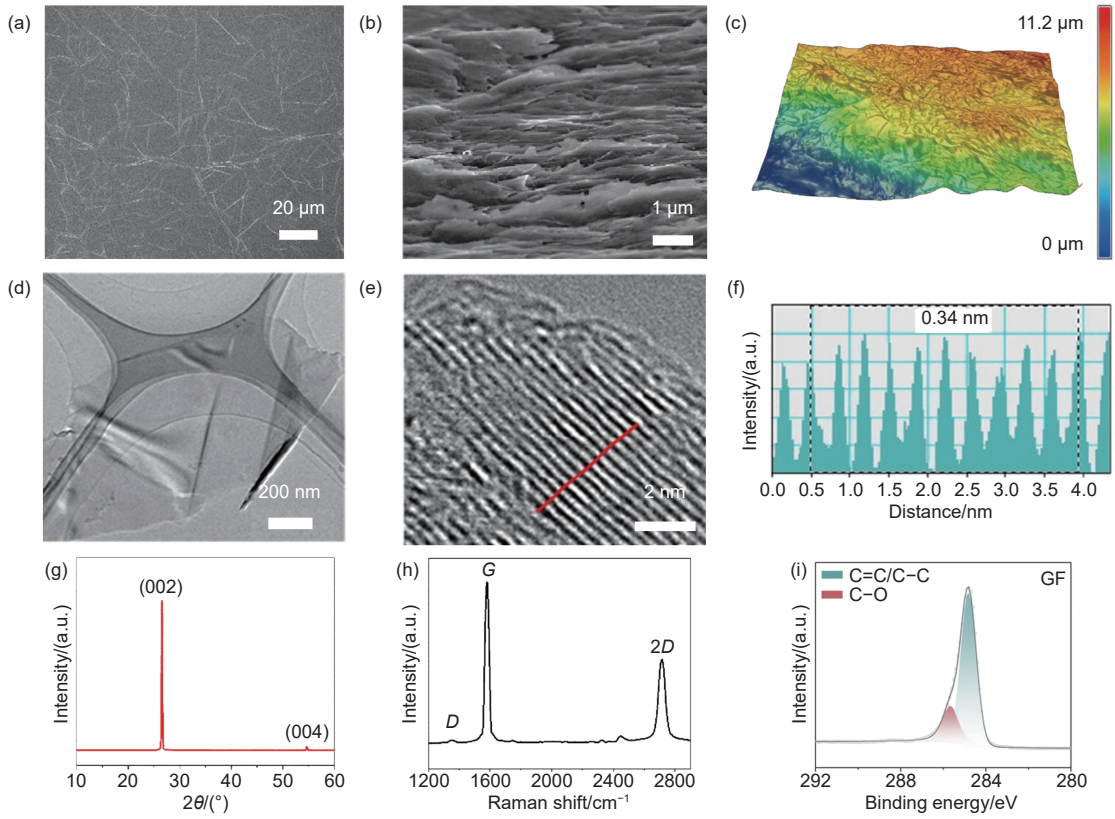

Fig. 3 (a) Surface SEM image of GAF (Reprinted with permission, Copyright 2023, Springer Nature)[75]. (b) Cross-sectional SEM image of GAF (Reprinted with permission, Copyright 2020, Elsevier)[76]. (c) The surface picture of GAF taken by a super-large depth of field 3D microscopic system (Reprinted with permission, Copyright 2023, Springer Nature)[75]. (d-e) HRTEM images at different magnifications of GAF. (f) The intensity profile along the red line in Fig. 3e (Reprinted with permission, Copyright 2024, American Chemical Society)[77]. (g) XRD pattern of GAF. (h) Raman spectrum of GAF. (i) XPS C1s spectrum of GAF (Reprinted with permission, Copyright 2023, Springer Nature)[75]

elemental ratios of oxygen in XPS. Collectively, these results validate that the thermally reduced GAF achieves low defect density, highly ordered stacking, and enhanced sp^2 domain continuity structural attributes that synergistically improve electrical conductivity, electrochemical activity, and mechanical robustness.

Fig. 4a demonstrates the feasibility of large-scale manufacturing of Graphene film (GF), which facilitates the industrial production of subsequent application products[78]. Fig. 4b reveals that the GF exhibits a tensile strength of 32 MPa, demonstrating robust mechanical properties suitable for diverse mechanical scenarios. As shown in Fig. 4c, the graphene film achieves the highest electrical conductivity among comparative carbon materials, measuring $(2.103 \pm 0.06) \times 10^6$ S m^{-1}. The inset small-angle X-ray scattering (SAXS) pattern in Fig. 4c displays a prism-like scattering profile, indicating an aligned hierarchical structure within the film. To validate the film's flexibility, repeated bending, rolling, and folding tests were conducted (Fig. 4d-f), with microscopic analysis confirming preserved microstructural integrity even under acute-angle folding (Fig. 4g). Remarkably, Fig. 4h demonstrates maintained resistivity stability through 100 000 bending cycles, highlighting its exceptional electrical durability for flexible electronic applications[78]. The comparative analysis in Fig. 4i underscores the graphene film's superior electrical conductivity over alternative materials, ensuring rapid electron transport essential for high performance electrochemical applications[79].

Graphene films, with their unique structures, play a crucial role in electrochemical reactions. It can be fabricated into diverse 3D structures such as hydrogels, aerogels, and foams through methods like hydrothermal/solvothermal reduction, chemical reduction, and electrochemical reduction. These 3D structures possess high specific surface areas, interconnected porous networks, and excellent electrical conductivity. In supercapacitors, they can be directly used as electrodes, showing high specific capacitances, good rate capabilities, and superior cycling stabilities. For example, the graphene hydrogel electrodes prepared by hydrothermal reduction exhibit excellent electrochemical performance[80]. In lithium-ion batteries (LIBs), the 3D graphene frameworks help with Li^+ diffusion and improve battery performance[81]. Composites of graphene with polymers, metals, or metal oxides further enhance the performance of electrochemical devices. In fuel cells, doped 3D graphene can enhance the electrocatalytic activity for the oxygen reduction reaction. Graphene films are also applied in sensing, enabling the detection of various substances with high sensitivity and selectivity. In summary, the unique structures of graphene films contribute to their outstanding performance in electrochemical energy storage, conversion, and sensing. However, challenges such as precise structure control and large-scale production still need to be addressed for further development.

4 Application of graphene films in the field of electrochemistry

Graphene films, owing to their tunable interlayer spacing, exceptionally high specific surface area (theoretical value: 2620 m^2 g^{-1}), and outstanding electrical conductivity (charge carrier mobility > 15 000 cm^2 V^{-1} s^{-1}), demonstrate revolutionary potential in electrochemical energy storage and sensing technologies. The following discussion elaborates on its transformative applications across 3 key domains: batteries, supercapacitors and electrochemical sensors[73–75].

4.1 Application of graphene films in batteries

The application of graphene films in the field of batteries not only improves the electrochemical performance of batteries, but also provides a new strategy in the field of LIBs safety due to their excellent thermal diffusion ability. The application of graphene films in batteries is driving energy storage technology innovation through their unique 2D structure and tunable physicochemical properties[81–85]. Consequently, Zhang et al. fabricated hyperboloidal graphene aerogels (HGA) by hydroplastic foaming (HPF) technology, constructing a high-porosity (> 85%) three-dimensional network through solvent-induced plasticization and oriented bubble growth mechanisms[74]. The

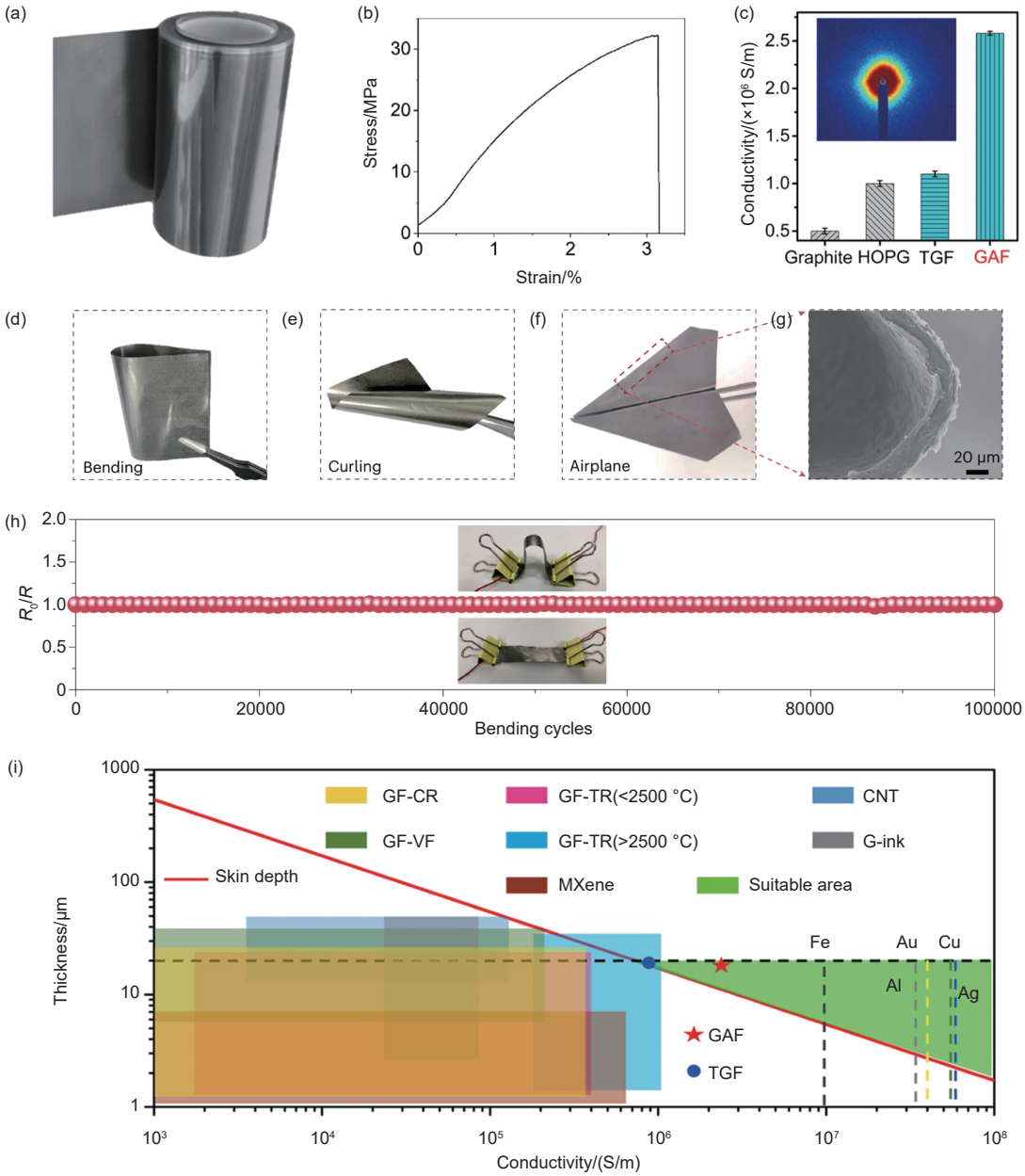

Fig. 4 (a) The photo of large-sized GF (Reprinted with permission, Copyright 2024, Springer Nature)[78]. (b) The stress-strain curve of GF (Reprinted with permission, Copyright 2023, Springer Nature)[75]. (c) A summary of conductivities of GAF, graphite, highly oriented pyrolytic graphite (HOPG), and typical flake size GO assembled film (TGF), the insert is SAXS pattern (Reprinted with permission, Copyright 2022, The National Academy of Sciences of the United States of America)[79]. Flexibility demonstrations under various deformation conditions: (d) bending, (e) curling and (f) folding into an airplane. (g) Cross-sectional SEM images of GAF folded at 180°. (h) Resistance alternation of GAF with 100 000 repeated bending tests (Reprinted with permission, Copyright 2024, Springer Nature)[78]. (i) Conductivity of GAF compared with other materials (Reprinted with permission, Copyright 2022, The National Academy of Sciences of the United States of America)[79]

paraffin-graphene composite (PGC) material, formed by combining hyperbolic graphene aerogel (HGA) derived from graphene oxide through a series of sophisticated fabrication processes with paraffin, demonstrates unique advantages in electrochemical applications (Fig. 5a). The PGC material exhibits not only high thermal conductivity but also exceptional electrical properties. When the graphene content exceeds 18.8%, the electrical conductivity of PGC surpasses 10^5 $S \cdot m^{-1}$, providing highly efficient pathways for electron transport. The superior conductivity of PGC effectively reduces the internal resistance of batteries, maximizes electron transport, accelerates ion diffusion, and enhances electrochemical reaction kinetics.

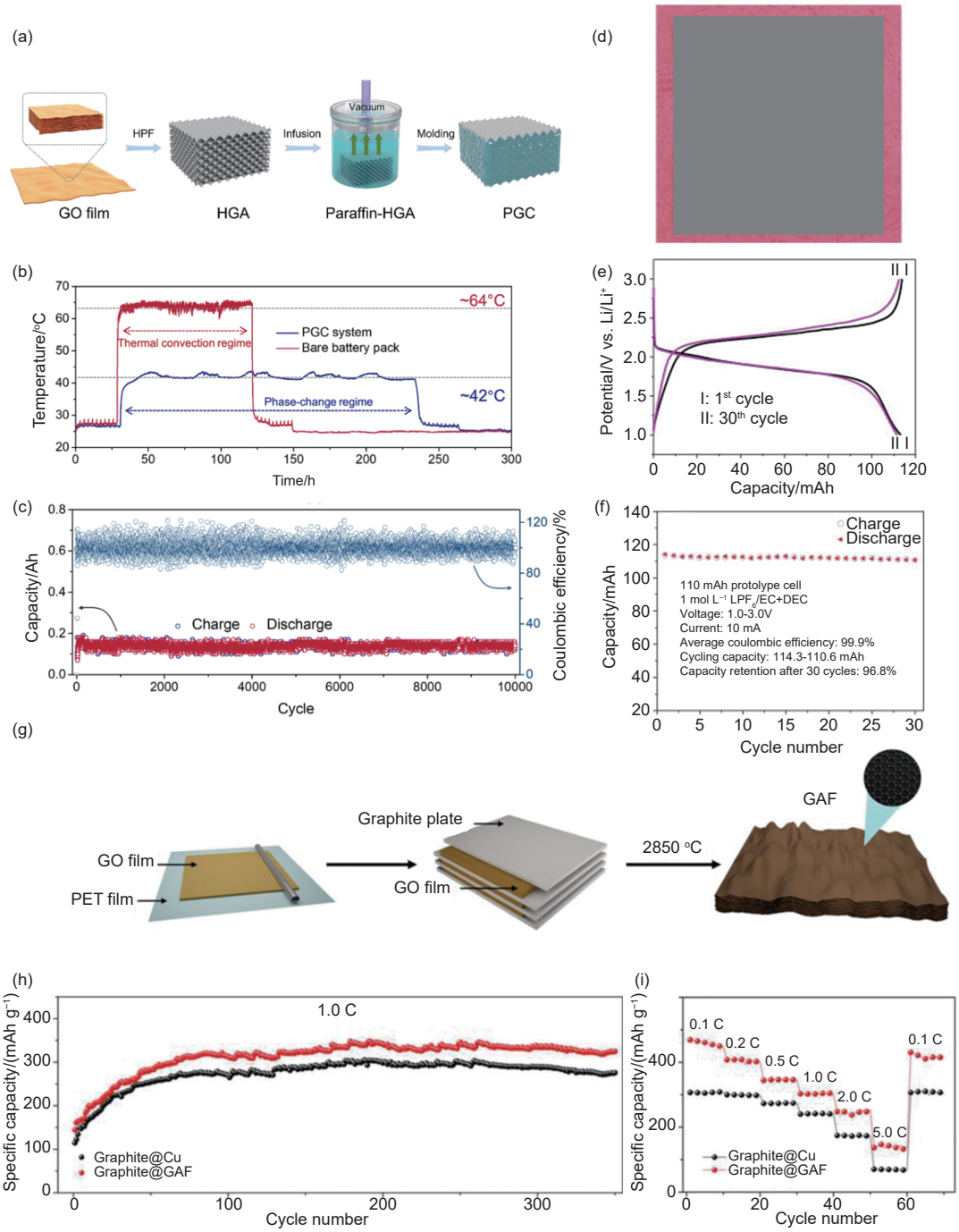

Fig. 5 (a) Fabrication and characteristic of PGC materials. (b) The temperature change of bare battery pack and PGC system during 10 000 charging-discharging cycles at 3 C rate. (c) The capacity and coulombic efficiency of battery pack with PGC system during 10 000 charging-discharging cycles (Reprinted with permission, Copyright 2025, Elsevier)[74]. (d) Photo of a sheet of G-PET film. Charge/discharge of cell between 3.0 and 1.0 V in 1 mol L^{-1} $LiPF_6$/EC + DEC at the current of 5 mA. (e) 1st and 30th cycles. (f) Cycling stability (Reprinted with permission, Copyright 2013, Elsevier)[86]. (g) Schematic of GAF fabrication procedure. (h) Cycling and (i) rate performances of graphite/GAF and graphite/Cu electrodes (Reprinted with permission, Copyright 2021, American Chemical Society)[87]

During long-term cycling tests, the battery module equipped with the PGC system maintained a stable temperature of ~ 42 °C under a current density of 3 C throughout 10 000 charge-discharge cycles, significantly lower than the 64 °C observed in bare battery modules cooled solely by thermal convection (Fig. 5b). Concurrently, the PGC-integrated system retained a high capacity retention rate of 93.3% (Fig. 5c). These improvements are attributed to the excellent electrical conductivity and structural stability

of PGC, which effectively suppresses irreversible side reactions within the battery, ensures electrochemical stability, and prolongs battery service life.

Beyond lithium-ion battery applications, graphene films also demonstrate remarkable potential in lithium-sulfur (Li-S) battery systems. Wang et al.'s research shows that graphene films perform outstandingly in the application of electrochemical reactions in Li-S batteries[86]. Fig. 5d shows the design of a metal-free cathode using a graphene-coated polyethylene terephthalate (G-PET) film as the current collector and sulfurized polyacrylonitrile (SPAN). This design leverages the properties of graphene to enhance battery performance. Fig. 5e-f present the excellent performance of Li-S batteries using G-PET films as current collectors. The assembled 110 mAh prototype battery has an energy density of 452 Wh kg^{-1}, and after 30 cycles at a 100% depth of discharge, the capacity retention rate is as high as 96.8%. This indicates that graphene films, as current collectors, effectively improve the energy density and cycling stability of batteries, showing promising application prospects in the field of lithium-sulfur batteries.

Complementing these advancements in battery component design, graphene's structural versatility has also enabled breakthroughs in flexible electrode fabrication. Zhao et al. prepared large-scale flexible electrodes (120 mm × 120 mm) through blade-coating film-forming of graphene aerogel film combined with high-temperature reduction (2850 °C) process. The 3D porous structure (porosity > 85%) and GAF has high conductivity ($(2.3 \pm 0.1) \times 10^5$ S m^{-1}), which significantly enhanced the mechanical adaptability of the electrodes (Fig. 5g-i)[87]. Electrochemical tests demonstrated that the GAF-based anode retained a capacity of 324 mAh g^{-1} after 350 cycles at 1 C (17.8% improvement), while maintaining a specific capacity of 141 mAh g^{-1} even at a high rate of 5 C. This performance enhancement was attributed to the 3D conductive network, which reduced interfacial charge transfer resistance by 58% and shortened Li^+ diffusion paths to less than 5 μm. The progressive capacity increase during the initial cycles (reaching 313 mAh g^{-1} after 75 cycles) revealed the sustained enhancement of electron transport facilitated by π-π interactions, providing theoretical guidance for developing flexible energy storage devices.

The interfacial optimization potential of graphene films has been further validated in mainstream battery configurations. Chen et al. found that graphene films are of great significance in the electrochemical reactions of LIBs[88]. Fig. 6a shows that the GAFs prepared by specific processes has an excellent structure and various excellent properties. Fig. 6b indicates that, taking the LFP battery as an example, when GF is used as the current collector, the battery exhibits excellent cycling performance at different rates, with a higher specific capacity retention rate at 5 C. This means that GF can reduce the interfacial resistance, dissipate heat efficiently, and improve the battery performance, showing great application potential.

While optimizing electrochemical interfaces, graphene innovations simultaneously address critical thermal safety challenges in advanced battery systems. Li et al. demonstrated a revolutionary breakthrough by employing graphene foil (Gr foil) as a novel current collector: The Gr foil fabricated by a continuous hot-pressing process exhibits an ultrahigh thermal conductivity of 1400.8 W m^{-1} K^{-1} (7-8 times that of Al/Cu foils) and an electrical conductivity of 1.3×10^6 S m^{-1} (Fig. 6c-f)[78]. In NCM811||graphite full-cell tests, the Gr||Gr system delivered an initial energy density of 271.9 Wh kg^{-1}, retaining 241.6 Wh kg^{-1} after 1000 cycles, while its 3D thermal network reduced local temperature gradients by 62%. Under extreme nail penetration conditions, the Gr foil achieved flame-free protection through structural stability at 800 °C, limiting gas evolution to 240 mmol (vs. 360 mmol in conventional systems), thereby fundamentally eliminating risks of thermite reactions and hydrogen evolution.

Graphene-based battery systems demonstrate transformative potential through innovations in thermal management, structural design, and dynamic interfaces. While advancements like adaptive 3D ar-

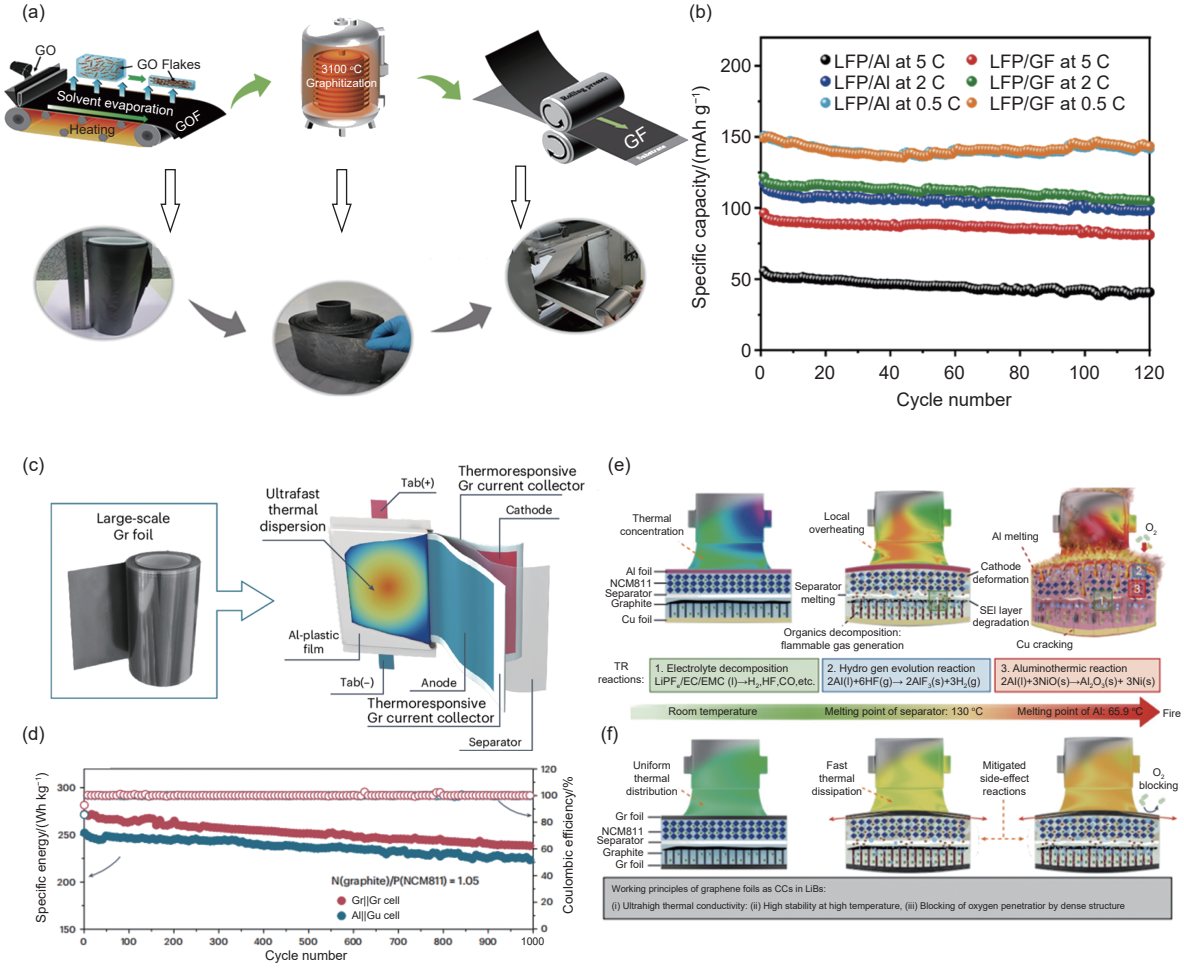

Fig. 6 (a) Schematic illustration of the roll-to-roll scale fabrication process of GF, with photographs of samples (bottom) and a schematic of the structural change from GOF to GF during graphitization (middle). (b) Cycling ability of LFP electrodes at different rates (Reprinted with permission, Copyright 2023, American Chemical Society)[88]. (c) Schematic diagram of a pouch cell integrated with Gr CCs. (d) Specific energy of pouch cells using Gr||Gr and Al||Cu foils over 1000 cycles at 1 C. (e) Incendiary explosion reaction mechanism of Al||Cu cells during thermal runaway (TR, thermal runaway; SEI, solid electrolyte interphase; EC, ethylene carbonate; EMC, ethyl methyl carbonate). (f) Safety improvement mechanism of Gr||Gr cells (Reprinted with permission, Copyright 2024, Springer Nature)[78]

chitectures and bio-inspired composites address dendrite suppression and stability, critical limitations persist: high energy-intensive manufacturing processes, nonlinear degradation of conductive networks during cycling, and unresolved multiphysics coupling under extreme operational conditions. Current research prioritizes multifunctional integration-transitioning from static material optimization to intelligent systems responsive to environmental stimuli. Challenges remain in balancing scalable production costs, long-term reliability under mechanical stress, and precise modeling of stress-capacity relationships in solid-state configurations, all while aligning with circular economy objectives for sustainable energy storage solutions.

4.2 Application of graphene film in supercapacitors

Because of its large specific surface area and excellent electron transport ability, graphene is an ideal electrode material for supercapacitors. Based on the intrinsic properties of graphene or its functionalization treatment can effectively improve the capacity density and cycle stability of capacitors, which provides favorable support for the development of high-performance capacitors. Supercapacitors are recognized as a promising energy storage solution in portable electronic devices due to their decent specific capacitance, high power density, rapid charge/discharge rates, and exceptional structural flexibility[89].

Graphene has been extensively applied in capacitor technologies, particularly in supercapacitors, highlighting its vast potential for energy storage applications through its unique combination of high surface area, superior electrical conductivity, and robust mechanical properties[90–91]. Research on graphene has entered a phase of rapid development, positioning it as a high-profile "star" material in advanced materials science, with its tunable layered structures (0D quantum dots to 3D composites) and stable electrochemical performance driving innovations in next-generation energy storage systems[92].

Zhang et al. demonstrated a composite film design based on MXene and reduced graphene oxide (rGO) (Fig. 7a-b)[93], where researchers achieved π-π conjugated interfacial coupling between MXene and rGO through a synergistic HCl/LiF etching and in-situ Zn foil reduction strategy. In this process, the electrostatic interactions between the —OH/—O functional groups on MXene surfaces and the negatively charged GO facilitated the formation of a stable suspension system. The synchronous chemical reduction process not only preserved the layered structure of the 2D materials but also established adjustable interlayer spacing (1.4-2.3 nm) by sulfuric acid molecule intercalation. This "electrode-electrolyte integrated" design shortened ion transport pathways to the nanoscale, enabling the composite electrode to maintain 93% capacity retention after 8000 cycles at 2 A cm^{-3} current density a 30% improvement over conventional carbon-based materials. They optimized the electrode-electrolyte integrated structure to provide a highly stable electrode substrate for subsequent rGO/carbon heterogeneous flexible Li-ion capacitors (LIC). Liu et al. developed flexible LIC employing self-supporting rGO/carbon heterostructures (Fig. 7c-d)[94], where an in-plane 3D interpenetrating network design eliminated conventional binder dependency. The innovation manifests in 2 aspects: (1) The cathode rGO/activated carbon and anode rGO/hard carbon achieve synergistic matching, balancing the electrode material's specific surface area (> 2000 $m^2 g^{-1}$) with Li^+ diffusion rate (10^{-8} $cm^2 s^{-1}$). (2) The PVDF-HFP/LiTFSI composite solid-state electrolyte enhances ion migration through polymer chain segment motion, enabling the device to maintain > 95% capacity retention over 10 000 cycles at an energy density of 0.94 mWh cm^{-2}. The incorporation of aluminum-laminate packaging technology further reduces the bending radius to 3 mm, providing a reliable power solution for wearable electronics. This work demonstrates significant progress in flexible energy storage through material-structure co-optimization strategies.

The integrated design of electrodes and electrolytes based on flexible Li-ion capacitors and three-dimensional interpenetrating network structure lay a foundation for the development of high energy density organic electrolyte hybrid energy storage system. Kung et al. addressed the challenge of volume expansion in conductive polymers through a covalently bonded system comprising sulfonated polyaniline and aminobenzoic acid-functionalized graphene, employing molecular-level interface engineering (Fig. 7e)[95]. The three-dimensional interpenetrating network structure achieved a specific capacitance of 642.6 F g^{-1}, representing a 2.4-fold enhancement compared to pristine polyaniline. Notably, the self-doping effect elevated the intrinsic electrical conductivity to 120 S cm^{-1}, while the mechanical confinement effect of the graphene framework extended the cycle life to 5000 cycles without capacitance decay. Remarkably, this system attained an energy density of 100.6 Wh kg^{-1} in organic electrolytes, surpassing the theoretical limit of aqueous supercapacitors. The collaborative optimization of material innovation and hybrid energy storage mechanism based on high energy density organic electrolyte system opens up a multi-dimensional linkage technology path for the design of new hybrid energy storage devices. The aqueous zinc-ion supercapacitor developed by Peng et al. ingeniously integrates the advantages of electric double-layer capacitance and battery-type energy storage through selective adsorption-induced self-assembly of the p-phenylenediamine modified holey graphene film (PPDA-HGF) cathode (Fig. 7f-g)[96]. The rapid adsorption/desorption of anions on the cathode surface

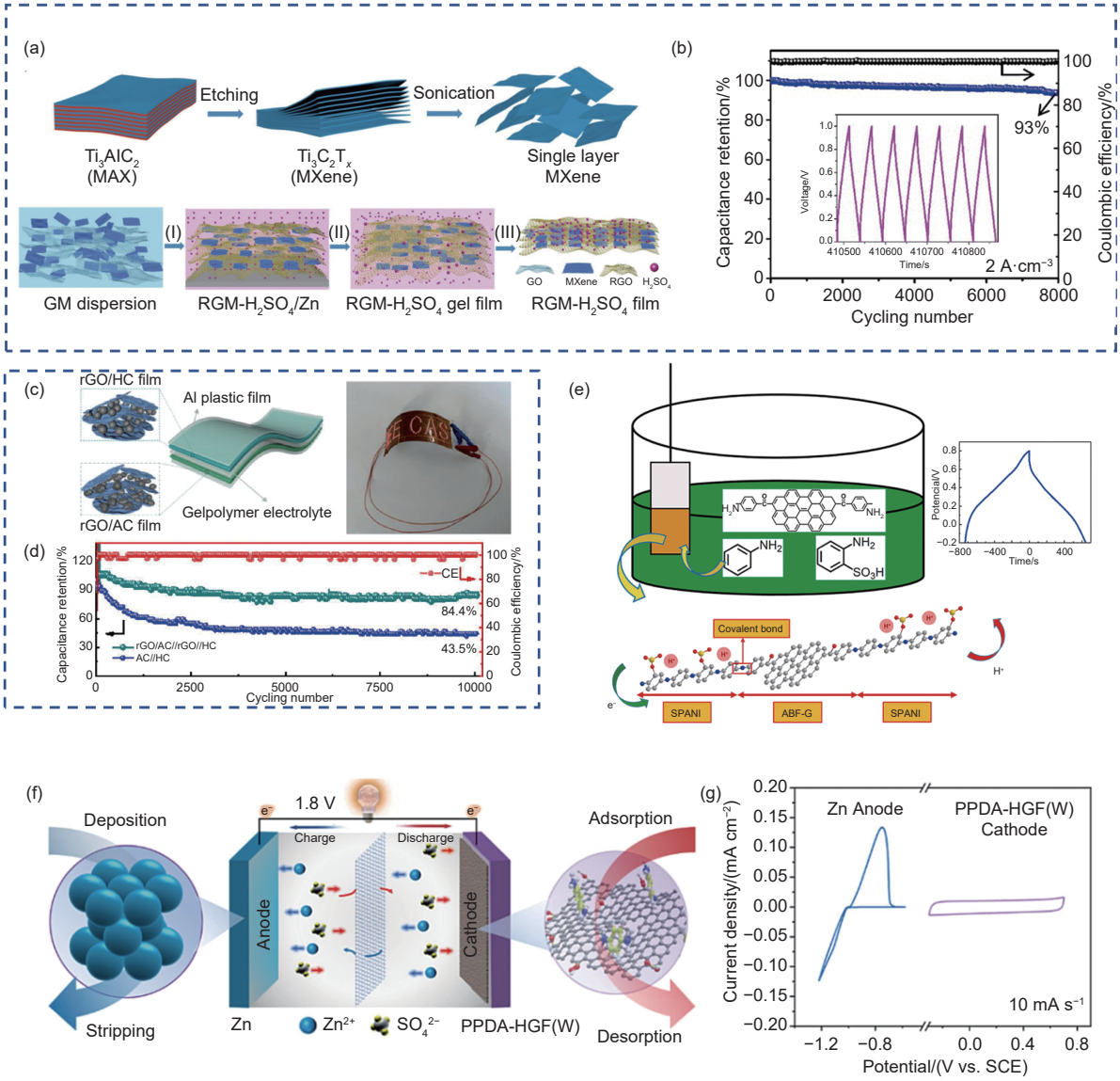

Fig. 7 (a) Schematic process of fabricating single layer MXene. (b) Cycling performance and coulombic efficiency of RGM30-H_2SO_4-based symmetric supercapacitor at a current density of 2 A cm^{-3} for 8000 cycles, inset shows GCD curves of the last seven cycles (Reprinted with permission, Copyright 2020, Springer Nature)[93]. (c) Fabrication of flexible quasi-solid-state rGO/AC//rGO/HC LIC pouch cell. (d) Cycling stability for AC//HC and rGO/AC//rGO/HC LICs (Reprinted with permission, Copyright 2023, Elsevier)[94]. (e) Electrochemical sensor based on SPANI and ABF-G for hydrogen ion (H^+) detection, along with a potential-time plot (Reprinted with permission, Copyright 2021, Elsevier)[95]. (f) Schematic diagram of the configuration and working mechanism of the AZISCs. (g) The CV curves of the PPDA-HGF(W) cathode and Zn anode measured at 10 mV s^{-1} (Reprinted with permission, Copyright 2023, Elsevier)[96]

(response time < 10 ms) combined with the reversible zinc deposition/stripping at the anode (Coulombic efficiency > 99.5%) enables the device to achieve both 28.6 Wh kg^{-1} energy density and 8.5 kW kg^{-1} power density. The coexistence of redox peaks at −1.2 V/−0.75 V (vs. SCE) in the CV curves with a rectangular electric double-layer response confirms the effectiveness of the hybrid energy storage mechanism. This configuration demonstrates exceptional electrochemical performance through synergistic collaboration between the Faradaic redox reactions and non-Faradaic processes.

Graphene-based supercapacitors show transformative advancements through innovative interfacial engineering and structural designs. While π-π coupled MXene composites and covalently bonded hybrid systems significantly enhance cycling stability and capacitance, challenges persist in suppressing interfacial side reactions, improving mechanical durability under extreme bending, and resolving safety concerns with

high-energy electrolytes. Current efforts focus on molecular-level interface optimization, synergistic storage mechanisms, and solid-state integration to advance wearable-compatible high-density energy systems.

4.3 Application of graphene film in electrochemical sensor

Benefiting from the high electrical conductivity, good mechanical properties and biocompatibility of graphene films, they break through the limitations of traditional electrode materials and provide a platform for a new generation of wearable sensors. With the development of society and the expansion of human activities, frequent cross-regional mobility has led to the global dissemination of pathogens. Consequently, rapid and accurate monitoring of physiological indicators becomes crucial for safeguarding human health. Electrochemical biosensors have garnered significant attention in environmental and health monitoring due to their high selectivity, sensitivity, cost-effectiveness, and miniaturization potential. By integrating the specificity of biorecognition with the sensitivity of electrochemical analysis, these sensors enable real-time monitoring of target analytes, playing a pivotal role in disease diagnosis, environmental surveillance, and clinical medicine[96–99]. However, conventional rigid electrodes (e.g., glassy carbon and gold electrodes) fail to meet the demands of wearable devices and flexible electronics, thereby limiting their advancement. To address this, Ji et al. developed graphene film-based electrodes for biosensing applications, which have high conductivity and good flexibility[75]. Thanks to the advantage of batch production of graphene films, they can achieve controllable and scalable fabrication of graphene based 3 electrode systems through laser engraving (Fig. 8a-b). The graphene film-based electrodes exhibit a wide linear range (1–200 μmol L^{-1}) and low limit of detection (LOD) (0.6 μmol L^{-1}) for dopamine detection (Fig. 8c-e), attributed to their high electron transfer rate and π-π interaction with dopamine. Graphene film-based electrode also have good biocompatibility. They modified the working electrode with glucose oxidase (GO_x) for glucose-specific detection. As shown in the calibration curves (Fig. 8f-g), the sensor exhibited a linear relationship between glucose concentration and reduction current at −0.48 V within 0.5–8.0 mmol L^{-1}, achieving a LOD of 0.41 mmol L^{-1}.

To further improve the detection capability of the electrode and meet the future demand for fast and sensitive detection. Ji et al. prepared graphene foam electrodes with superior surface roughness, internal porosity, and rich wrinkled microstructures[100]. Thanks to the structural characteristics of the graphene foam electrode, the contact between the electrode and the electrolyte was enhanced, and the charge transfer is promoted, thus significantly improving the electrocatalytic activity of the sensor for glucose oxidation. As illustrated in Fig. 8h, chronoamperometric measurements demonstrate a linear detection range for glucose spanning 0.5 to 1 mmol L^{-1} (Fig. 8i). Selective testing by i-t methodology under co-existing biomolecular conditions reveals distinct current responses upon glucose addition, confirming the electrode's excellent selectivity (Fig. 8j).

Additionally, Wang et al. fully leveraged graphene's exceptional electrical conductivity and abundant functional groups to engineer a multifunctional bilayer film structure using graphene as the raw material through bar-coating techniques and oxygen content modulation methods. This bilayer structure demonstrates unique electron-proton coupling characteristics, enabling sensitive responses to ultraviolet radiation, temperature variations, and humidity changes (Fig. 8k-m). The graphene multilayer film achieves continuous monitoring under simultaneous exposure to these three environmental factors (Fig. 8n). The team further demonstrated the practical application of GO/rGO multifunctional wearable sensors in artificial intelligence (AI) systems for detecting kitchen environmental changes (Fig. 8o), providing novel insights for designing advanced wearable devices such as electronic skins and human-machine interaction systems[101].

Graphene-based electrochemical sensors achieve

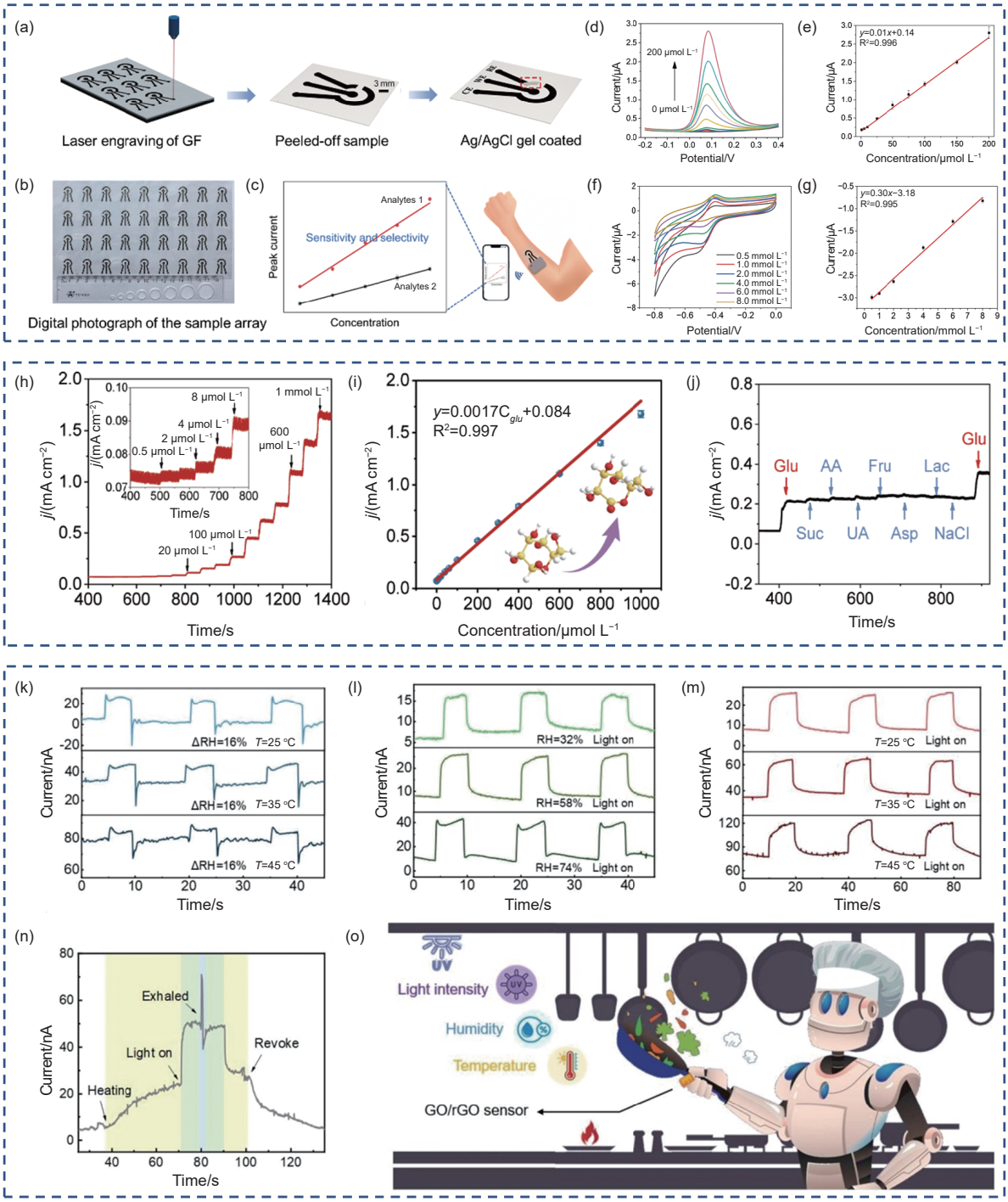

Fig. 8 (a) Schematic illustration showing the laser engraving process on GAF to fabricate GAF-based 3-electrode system. (b) Digital photograph showing the as-prepared electrode array. (c) Schematic diagram of the wearable electrode for portable electrochemical detection. (d) DPV curves measured with different concentrations of DA using the GAF-based electrode. (e) The fitted calibration curve of the GAF-based electrode between the peak currents and DA concentrations. (f) CV curves of Nafion/GO_x/GAF electrode in PBS buffer with different glucose concentrations (scan rate = 0.1 V s^{-1}). (g) The fitted calibration curve of the Nafion/GO_x/GAF electrode between the cathodic peak intensities and concentrations of glucose (Reprinted with permission, Copyright 2023, Springer Nature)[75]. (h) Amperometric responses of Ni/GFM with successive injection of glucose (0.5 μmol L^{-1}-1 mmol L^{-1}) at 0.55 V (inset: enlarged plot in the range from 400 to 800 s). (i) Linear curve peak of current density versus glucose concentrations for Ni/GFM. (j) Amperometric responses of Ni/GFM with continuous addition of glucose (1 mmol L^{-1}) and other interfering substances (0.1 mmol L^{-1}) (Reprinted with permission, Copyright 2024, Elsevier)[100]. (k) Current changes of the device on different temperature heating plates with multiple increases in surface humidity (ΔRH = 16%). (l) Current changes due to multiple light exposure when the device is placed in different humidity environments. (m) Current changes caused by multiple light exposure when the device is placed on different temperature heating plates. (n) Current changes of the device under three simultaneous environmental variations, from application to removal. (o) Application of the GO/rGO bilayer film device in future smart kitchen robots (Reprinted with permission, Copyright 2025, Elsevier)[101]

breakthroughs by integrating conductivity, flexibility, and biocompatibility. Innovations like laser-structured electrodes enable wide-range biomolecule detection, while graphene foam enhances sensitivity and selectivity in complex environments. Smart bilayer systems coupled with AI demonstrate multifunctional environmental monitoring. Key challenges involve improving batch consistency, anti-interference capability in biofluids, and mechanical endurance. Advancements focus on microstructural optimization, AI-enhanced multimodal analysis, and self-healing designs to drive precision wearable sensing technologies.

5 Conclusions and outlook

Based on the aforementioned research progress, we have analyzed various preparation methods of graphene assembled films, with a focused investigation on the microstructure, morphology, and physical properties of graphene films prepared by high-temperature thermal reduction. We then thoroughly discussed the primary applications of graphene assembled films in electrochemical fields such as batteries, supercapacitors, and electrochemical sensors. Benefiting from their lightweight flexibility, high conductivity, large specific surface area, and superior mechanical properties, graphene films exhibit unique advantages in these domains. Their flexible nature enables repeated 180° bending without damaging conductive networks; the dual advantages of high conductivity and thermal conductivity surpass the performance limits of traditional metallic materials; hierarchical porous structures and tunable surface chemistry provide precise platforms for interfacial engineering in electrochemical reactions. Furthermore, with the advent of the AI era, the deep coupling of AI big models with automated experimental technology has led to the evolution of graphene assembled films from passive functional materials to active intelligent systems. By using AI, experimental data can be extensively analyzed and reasonable models can be predicted, which can effectively monitor electrochemical and microenvironmental changes, providing more extensive applications and fast, data-driven insights for graphene assembled films. These achievements not only drive transformative advancements in flexible electronics, high energy density storage systems, and smart sensing technologies but also establish a material science foundation for redefining design paradigms in next-generation electrochemical devices. Despite these advantages, significant challenges remain for widespread electrochemical applications: First, the conductivity of graphene films still lags behind the theoretical limit of pristine graphene, which may hinder electron transport in electrode applications. Second, the near-complete removal of oxygen-containing functional groups during thermal reduction renders the surface chemically inert, complicating surface modification with active materials and compromising their stability. Third, while graphene films demonstrate adequate mechanical strength and flexibility, further enhancement is required to withstand complex bending conditions in wearable devices. Addressing these challenges will expand graphene assembled films' electrochemical applications and potentially establish them as universal electrode substrates in the field.

Conflict of interest

The authors declare that they have no conflict of interest.

Acknowledgements

The authors sincerely acknowledge financial support from the National Natural Science Foundation of China (22279097), the Key R&D Program of Hubei Province (2023BAB103), the PhD Scientific Research and Innovation Foundation of The Education Department of Hainan Province Joint Project of Sanya Yazhou Bay Science and Technology City (HSPHDSRF-2024-03-022).

Author information

***Corresponding author:**

LIU Bo, Ph.D. E-mail: liubo2024@whut.edu.cn;

HE Da-ping, Professor. E-mail: hedaping@whut.edu.cn

First author:

† ZHU Yong-fang and † JI Xiao-dong contributed equally to this work.

References

[1] Jiang H. Chemical preparation of graphene-based nanomaterials and their applications in chemical and biological sensors[J]. Small, 2011, 7(17): 2413-2427.

[2] Wang Y, Luo J, Lu Z, et al. A review of the high-concentration processing, densification, and applications of graphene oxide and graphene[J]. New Carbon Materials, 2024, 39(3): 483-505.

[3] Yang S, Cao Y, He Y, et al. A review of the use of graphene-based materials in electromagnetic-shielding[J]. New Carbon Materials, 2024, 39(2): 223-239.

[4] Chen Z, Ren J, Qiao J, et al. Influence of functionalized graphene on the bacterial and fungal diversity of vicia faba rhizosphere soil[J]. New Carbon Materials, 2024, 39(6): 1227-1242.

[5] Bhaiyya M L, Pattnaik P K, Goel S. Miniaturized electrochemiluminescence platform with laser-induced graphene-based single electrode for interference-free sensing of dopamine, xanthine, and glucose[J]. IEEE Transactions on Instrumentation and Measurement, 2021, 70: 1-8 DOI: 10.1109/TIM.2021.3071215 .

[6] Low C, Walsh F, Chakrabarti M, et al. Electrochemical approaches to the production of graphene flakes and their potential applications[J]. Carbon, 2013, 54: 1-21.

[7] Sundaram R S, Gómez-Navarro C, Balasubramanian K, et al. Electrochemical modification of graphene[J]. Advanced Materials, 2008, 20(16): 3050-3053.

[8] Tang L, Wang Y, Li Y, et al. Preparation, structure and electrochemical properties of reduced graphene sheet films[J]. Advanced Functional Materials, 2009, 19(17): 2782-2789.

[9] Chen K, Song S, Liu F, et al. Structural design of graphene for use in electrochemical energy storage devices[J]. Chemical Society Reviews, 2015, 44(17): 6230-6257.

[10] Umar E, Ikram M, Haider J, et al. 3D graphene-based material: overview, perspective, advancement, energy storage, biomedical engineering and environmental applications a bibliometric analysis[J]. Journal of Environmental Chemical Engineering, 2023, 11(5): 110339.

[11] Hou J, Shao Y, Ellis M W, et al. Graphene-based electrochemical energy conversion and storage: fuel cells, supercapacitors and lithium ion batteries[J]. Physical Chemistry Chemical Physics, 2011, 13(34): 15384-15402.

[12] Tang Q, Zhou Z, Chen Z. Graphene-related nanomaterials: tuning properties by functionalization[J]. Nanoscale, 2013, 5(11): 4541-4583.

[13] Chakrabarti M, Low C, Brandon N, et al. Progress in the electrochemical modification of graphene-based materials and their applications[J]. Electrochimica Acta, 2013, 107: 425-440.

[14] Farjadian F, Abbaspour S, Sadatlu M A A, et al. Recent developments in graphene and graphene oxide: properties, synthesis, and modifications: a review[J]. ChemistrySelect, 2020, 5(33): 10200-10219.

[15] Liu J, Tang J, Gooding JJ. Strategies for chemical modification of graphene and applications of chemically modified graphene[J]. Journal of Materials Chemistry, 2012, 22(25): 12435-12452.

[16] Xu C, Xu B, Gu Y, et al. Graphene-based electrodes for electrochemical energy storage[J]. Energy & Environmental Science, 2013, 6(5): 1388-1414 DOI: 10.1039/C3EE23870A.

[17] Shen J, Hu Y, Li C, et al. Layer-by-layer self-assembly of graphene nanoplatelets[J]. Langmuir, 2009, 25(11): 6122-6128.

[18] Tian W, VahidMohammadi A, Wang Z, et al. Layer-by-layer self-assembly of pillared two-dimensional multilayers[J]. Nature Communications, 2019, 10(1): 2558.

[19] De Villiers M M, Otto D P, Strydom S J, et al. Introduction to nanocoatings produced by layer-by-layer (LBL) self-assembly[J]. Advanced Drug Delivery Reviews, 2011, 63(9): 701-715.

[20] Ang A S M, Berndt C C. A review of testing methods for thermal spray coatings[J]. International Materials Reviews, 2014, 59(4): 179-223.

[21] Amin S, Panchal H. A review on thermal spray coating processes[J]. International Journal of Current Trends in Engineering & Research, 2016, 2(4): 556-563.

[22] Moridi A, Hassani-Gangaraj S M, Guagliano M, et al. Cold spray coating: review of material systems and future perspectives[J]. Surface Engineering, 2014, 30(6): 369-395.

[23] Hu Z, Zhao Y, Zou W, et al. Doping of graphene films: open the way to applications in electronics and optoelectronics[J]. Advanced Functional Materials, 2022, 32(42): 2203179.

[24] Yang X, Zheng X, Li H, et al. Non-noble-metal catalyst and Zn/graphene film for low-cost and ultra-long-durability solid-state Zn-air batteries in harsh electrolytes[J]. Advanced Functional Materials, 2022, 32(31): 2200397.

[25] Jin S, Gao Q, Zeng X, et al. Effects of reduction methods on the structure and thermal conductivity of free-standing reduced graphene oxide films[J]. Diamond and Related Materials, 2015, 58: 54-61.

[26] Huang S Y, Zhao B, Zhang K, et al. Enhanced reduction of graphene oxide on recyclable cu foils to fabricate graphene films with superior thermal conductivity[J]. Scientific Reports, 2015, 5(1): 14260.

[27] Zhang D, Tong J, Xia B. Humidity-sensing properties of chemically reduced graphene oxide/polymer nanocomposite film sensor based on layer-by-layer nano self-assembly[J]. Sensors and Actuators B: Chemical, 2014, 197: 66-72.

[28] Niu Y, Zhao J, Zhang X, et al. Large area orientation films based on graphene oxide self-assembly and low-temperature thermal reduction[J]. Applied Physics Letters, 2012, 101(18): 181903.

[29] Chen C, Yang Q, Yang Y, et al. Self-assembled free-standing graphite oxide membrane[J]. Advanced Materials, 2009, 21(29): 3007-3011.

[30] Jia K, Zhang J, Zhu Y, et al. Toward the commercialization of

chemical vapor deposition graphene films[J]. Applied Physics Reviews, 2021, 8(4): 041306

[31] Xu Z, Gao C. Graphene in macroscopic order: liquid crystals and wet-spun fibers[J]. Accounts of Chemical Research, 2014, 47(4): 1267-1276.

[32] Parlak O, Tiwari A, Turner A P, et al. Template-directed hierarchical self-assembly of graphene based hybrid structure for electrochemical biosensing[J]. Biosensors and Bioelectronics, 2013, 49: 53-62.

[33] Wei W, Vekariy R L, You C, et al. Concisely modularized assembling of graphene-based thin films with promising electrode performance[J]. Materials Chemistry Frontiers, 2019, 3(7): 1462-1470.

[34] Bittinger S C, Struck J, Dobschall F, et al. Nanocomposites of titania/reduced graphene oxide: flexible humidity sensors tuned via photocatalytic reduction[J]. ACS Applied Nano Materials, 2025, 8(15): 7428-7439.

[35] Zeng Y, Li T, Yao Y, et al. Thermally conductive reduced graphene oxide thin films for extreme temperature sensors[J]. Advanced Functional Materials, 2019, 29(27): 1901388.

[36] Pavlou C, Koutroumanis N, Manikas A C, et al. Highly efficient, electro-thermal heater based on marangoni-driven, oriented reduced graphene oxide/poly (ether imide) nanolaminates[J]. ACS Applied Materials & Interfaces, 2024, 17(1): 2000-2009 DOI: 10.1021/acsami.4c17273.

[37] Guo S, Chen J, Zhang Y, et al. Graphene-based films: fabrication, interfacial modification, and applications[J]. Nanomaterials, 2021, 11(10): 2539.

[38] Sheath P, Majumder M. Flux accentuation and improved rejection in graphene-based filtration membranes produced by capillary-force-assisted self-assembly[J]. Philosophical Transactions of the Royal Society A: Mathematical, Physical and Engineering Sciences, 2016, 374(2060): 20150028.

[39] Tkacz R, Oldenbourg R, Fulcher A, et al. Capillary-force-assisted self-assembly (cas) of highly ordered and anisotropic graphene-based thin films[J]. The Journal of Physical Chemistry C, 2014, 118(1): 259-267.

[40] Shim J, Yun J M, Yun T, et al. Two-minute assembly of pristine large-area graphene based films[J]. Nano Letters, 2014, 14(3): 1388-1393.

[41] Joshi R, Narayanaswamy M P, Sinha S, et al. Reduced-graphene-oxide-based thin films: an alternative coating for harsh space environments[J]. ACS Applied Materials & Interfaces, 2024, 16(50): 69690-69702 DOI: 10.1021/acsami.4c11126.

[42] Novoa-De León IC, Johny J, Vázquez-Rodríguez S, et al. Nanocarbon hybrid films of reduced graphene oxide and n-doped graphene quantum dots as a metal-free platform for graphene-enhanced raman scattering[J]. ACS Applied Materials & Interfaces, 2025, 17,11: 17251-17259 DOI: 10.1021/acsami.4c21874.

[43] Khlaifia D, Aouassa M, Torrisi L, et al. RGO-Si QDs hybrid photodetector with enhanced photosensitivity[J]. Physica B: Condensed Matter, 2025, 706: 417133.

[44] Guan K, Shen J, Liu G, et al. Spray-evaporation assembled graphene oxide membranes for selective hydrogen transport[J]. Separation and Purification Technology, 2017, 174: 126-135.

[45] Peng L, Xu Z, Liu Z, et al. Ultrahigh thermal conductive yet superflexible graphene films[J]. Advanced Materials, 2017, 29(27): 1700589.

[46] Arslan H K, Shekhah O, Wohlgemuth J, et al. High-throughput fabrication of uniform and homogenous mof coatings[J]. Advanced Functional Materials, 2011, 21(22): 4228-4231.

[47] Bhattacharjee J, Roy S, Shaikh A A, et al. Efficient fabrication and characterization of doped nanocomposites for thermoelectric materials[J]. Nano Trends, 2025, 10: 100109 DOI: 10.1016/j.nwnano.2025.100109

[48] Zhou C, Gao H, Bu S, et al. Principles for fabricating moisture barrier films via stacked janus graphene layers[J]. Nature Communications, 2025, 16(1): 3512.

[49] Tsou C H, An Q F, Lo S C, et al. Effect of microstructure of graphene oxide fabricated through different self-assembly techniques on 1-butanol dehydration[J]. Journal of Membrane Science, 2015, 477: 93-100.

[50] Robinson J T, Zalalutdinov M, Baldwin J W, et al. Wafer-scale reduced graphene oxide films for nanomechanical devices[J]. Nano Letters, 2008, 8(10): 3441-3445.

[51] Guo Y, Di C, Liu H, et al. General route toward patterning of graphene oxide by a combination of wettability modulation and spin-coating[J]. ACS Nano, 2010, 4(10): 5749-5754.

[52] Gilje S, Han S, Wang M, et al. A chemical route to graphene for device applications[J]. Nano Letters, 2007, 7(11): 3394-3398.

[53] Li W, Lv F, Xi J, et al. A novel mxene/go thermoacoustic loudspeaker with high sound pressure[J]. IEEE Sensors Journal, 2025, 25 (11): 19359 − 19366 DOI: 10.1109/JSEN.2025.3558925

[54] Zhang G, Shaffer C E, Wang C Y, et al. Effects of non-uniform current distribution on energy density of li-ion cells[J]. Journal of The Electrochemical Society, 2013, 160(11): A2299-A2305.

[55] Cao X, Qi D, Yin S, et al. Ambient fabrication of large-area graphene films via a synchronous reduction and assembly strategy[J]. Advanced Materials, 2013, 25(21): 2957-2962.

[56] Ibarra-Barreno C M, Chowdhury S, Crosta M, et al. Bottom-up fabrication of B,N-doped graphene electrodes from thiol-terminated borazine molecules working in solar cells[J]. ACS Applied Materials & Interfaces, 2025, 17: 23062-23075 DOI: 10.1021/acsami.4c23116.

[57] Lv H, Wu L, Du C, et al. Graphene oxide/Ni/carbon nanocoils synergizing dielectric/magnetic/chiral multiple losses for weather-resistant electromagnetic protective application[J]. Chemical Engineering Journal, 2025, 512: 162263 DOI: 10.1016/j.cej.2025.162263

[58] Seon Lee Y, Ryeol Kim N, Ki Park S, et al. Effects of high-temperature thermal reduction on thermal conductivity of reduced graphene oxide polymer composites[J]. Applied Surface Science, 2024, 650: 159140.

[59] Liu K, Ren E, Ma J, et al. Controllable preparation of graphene-based film deposited on cemented carbides by chemical vapor deposition[J]. Journal of Materials Science, 2020, 55(10): 4251-4264.

[60] Yan K, Fu L, Peng H, et al. Designed CVD growth of graphene via process engineering[J]. Accounts of Chemical Research, 2013, 46(10): 2263-2274.

[61] Yin W, Liu C, Li J. A review on high-efficiency transfer of graphene films free from defects and contamination[J]. Energy & Environmental Materials, 2025: e70009.

[62] Li X, Colombo L, Ruoff RS. Synthesis of graphene films on copper foils by chemical vapor deposition[J]. Advanced Materials, 2016, 28(29): 6247-6252.

[63] Kumar S, Goswami M, Singh N, et al. Flexible and lightweight graphene grown by rapid thermal processing chemical vapor deposition for thermal management in consumer electronics[J]. New Carbon Materials, 2023, 38(3): 534-540.

[64] Edwards R S, Coleman K S. Graphene film growth on polycrystalline metals[J]. Accounts of Chemical Research, 2013, 46(1): 23-30.

[65] Liu X, Xu Q, Zhang X, et al. Fabrication of strain-sensing fibers with silver nanoparticles and reduced graphene oxide via wet spinning[J]. Nanotechnology, 2025, 36(10): 105501.

[66] Cheng X, Tian X, Liao S, et al. Wet spinning for high-performance fiber supercapacitor based on Fe-doped MnO_2 and graphene[J]. Carbon, 2024, 230: 119572.

[67] Huang T, Chu X, Cai S, et al. Tri-high designed graphene electrodes for long cycle-life supercapacitors with high mass loading[J]. Energy Storage Materials, 2019, 17: 349-357.

[68] Ambade R B, Lee K H, Kang D J, et al. Advances in porous graphene and scalable wet-spinning fiber assembly[J]. Accounts of Materials Research, 2022, 4(5): 389-402 DOI: 10.1021/accountsmr.2c00186.

[69] Cong H P, Ren X C, Wang P, et al. Wet-spinning assembly of continuous, neat and macroscopic graphene fibers[J]. Scientific reports, 2012, 2(1): 613.

[70] Liu Z, Li Z, Xu Z, et al. Wet-spun continuous graphene films[J]. Chemistry of Materials, 2014, 26(23): 6786-6795.

[71] Xu Z, Gao C. Graphene chiral liquid crystals and macroscopic assembled fibres[J]. Nature Communications, 2011, 2(1): 571.

[72] Ren W, Qian W, Zhang Z, et al. Intercross-linked aramid nanofibers/graphene hybrid films toward high mechanical strength and electrical conductivity[J]. Journal of Alloys and Compounds, 2024, 976: 173390.

[73] Zhang H, Xing J, Wei G, et al. Electrostatic-induced ion-confined partitioning in graphene nanolaminate membrane for breaking anion–cation co-transport to enhance desalination[J]. Nature Communications, 2024, 15(1): 4324.

[74] Zhang C, Mao Y, Li K, et al. High power and energy density graphene phase change composite materials for efficient thermal management of li-ion batteries[J]. Energy Storage Materials, 2025, 75: 104003.

[75] Ji X, Zhao X, Zhang Z, et al. Scalable fabrication of graphene-assembled multifunctional electrode with efficient electrochemical detection of dopamine and glucose[J]. Nano Research, 2023, 16(5): 6361-6368.

[76] Fu H, Xiao Y, Song R, et al. Rapid soldering of flexible graphene assembled films at low temperature in air with ultrasonic assistance[J]. Carbon, 2020, 158: 55-62.

[77] Luo Z, Li P, Xin Y, et al. Dual-circularly polarized and flexible metasurface antenna based on graphene assembled film for satellite communications[J]. ACS Applied Materials & Interfaces, 2024, 16(13): 16724-16731 DOI: 10.1021/acsami.4c01211.

[78] Li L, Yang J, Tan R, et al. Large-Scale current collectors for regulating heat transfer and enhancing battery safety[J]. Nature Chemical Engineering, 2024, 1(8): 542-551.

[79] Song R, Mao B, Wang Z, et al. Comparison of copper and graphene-assembled films in 5G wireless communication and thz electromagnetic-interference shielding[J]. Proceedings of the National Academy of Sciences, 2023, 120(9): e2209807120.

[80] Xu Y, Shi G, Duan X. Self-assembled three-dimensional graphene macrostructures: synthesis and applications in supercapacitors[J]. Accounts of Chemical Research, 2015, 48(6): 1666-1675.

[81] Shehzad K, Xu Y, Gao C, et al. Three-dimensional macro-structures of two-dimensional nanomaterials[J]. Chemical Society Reviews, 2016, 45(20): 5541-5588.

[82] Brownson D A, Banks C E. Graphene electrochemistry: an overview of potential applications[J]. Analyst, 2010, 135(11): 2768-2778.

[83] Brownson D A, Kampouris D K, Banks C E. Graphene electrochemistry: fundamental concepts through to prominent applications[J]. Chemical Society Reviews, 2012, 41(21): 6944-6976.

[84] Feng X, Li R, Ma Y, et al. One-step electrochemical synthesis of graphene/polyaniline composite film and its applications[J]. Advanced Functional Materials, 2011, 21(15): 2989-2996.

[85] Vashist S K, Luong J H. Recent advances in electrochemical biosensing schemes using graphene and graphene-based nanocomposites[J]. Carbon, 2015, 84: 519-550.

[86] Wang L, He X, Li J, et al. Graphene-coated plastic film as current collector for lithium/sulfur batteries[J]. Journal of Power Sources, 2013, 239: 623-627.

[87] Zhao Y, Yang J, Ma J, et al. Highly reduced graphene assembly film as current collector for lithium ion batteries[J]. ACS Sustainable Chemistry & Engineering, 2021, 9(25): 8635-8641 DOI: 10.1021/acssuschemeng.1c02414.

[88] Chen S, Wang Q, Liu C, et al. Roll-to-roll scale fabrication of high-performance graphene-assembled film cathode current collectors for lithium-ion batteries[J]. ACS Sustainable Chemistry & Engineering, 2023, 11(36): 13483-13491 DOI: 10.1021/acssuschemeng.3c03939.

[89] Azman N H N, Mamat Mat Nazir MS, Ngee L H, et al. Graphene-based ternary composites for supercapacitors[J]. International

Journal of Energy Research, 2018, 42(6): 2104-2116.

[90] Iqbal M F, Yousef A K, Hassan A, et al. Significantly improved electrochemical characteristics of nickel sulfide nanoplates using graphene oxide thin film for supercapacitor applications[J]. Journal of Energy Storage, 2021, 33: 102091.

[91] Mohamed N B, El-Kady M F, Kaner R B. Macroporous graphene frameworks for sensing and supercapacitor applications[J]. Advanced Functional Materials, 2022, 32(42): 2203101.

[92] Ke Q, Wang J. Graphene-based materials for supercapacitor electrodes–a review[J]. Journal of Materiomics, 2016, 2(1): 37-54.

[93] Zhang M, Cao J, Wang Y, et al. Electrolyte-mediated dense integration of graphene-mxene films for high volumetric capacitance flexible supercapacitors[J]. Nano Research, 2021, 14(3): 699-706.

[94] Liu W, An Y, Wang L, et al. Mechanically flexible reduced graphene oxide/carbon composite films for high-performance quasi-solid-state lithium-ion capacitors[J]. Journal of Energy Chemistry, 2023, 80: 68-76.

[95] Kung C Y, Wang T L, Lin H Y, et al. A high-performance covalently bonded self-doped polyaniline–graphene assembly film with superior stability for supercapacitors[J]. Journal of Power Sources, 2021, 490: 229538.

[96] Peng L, Liu Z, Liu Z, et al. Optimization strategy of molecular modified graphene films for high-performance aqueous zinc-ion hybrid supercapacitors[J]. Journal of Electroanalytical Chemistry, 2023, 949: 117850.

[97] Zheng D, Hu H, Liu X, et al. Application of graphene in elctrochemical sensing[J]. Current Opinion in Colloid & Interface Science, 2015, 20(5-6): 383-405 DOI: doi.org/10.1016/j.cocis.2015.10.011.

[98] Gan T, Hu S. Electrochemical sensors based on graphene materials[J]. Microchimica Acta, 2011, 175: 1-19.

[99] Wu S, He Q, Tan C, et al. Graphene-based electrochemical sensors[J]. Small, 2013, 9(8): 1160-1172.

[100] Ji X, Jin H, Qian W, et al. Flexible, scalable hierarchical graphene foam decorated with nickel layer for highly sensitive enzyme-free glucose sensing[J]. Journal of Alloys and Compounds, 2024, 1004: 175902.

[101] Wang L, Wang T, Li Y, et al. Graphene bilayer film responsive to ultraviolet, humidity, and temperature[J]. Chemical Engineering Journal, 2025, 505: 159460.

石墨烯组装膜作为电化学反应平台的研究进展

朱永芳[1,2,†]，吉晓东[1,2,†]，潘文凯[1,2]，吴 耕[1]，李 鹏[3]，刘 波[1,3,*]，何大平[1,2,3,*]

（1. 武汉理工大学 三亚科教创新园，海南 三亚 572000；
2. 武汉理工大学 材料科学与工程学院，湖北 武汉 430070；
3. 武汉理工大学 物理与力学学院湖北省射频微波应用工程中心，湖北 武汉 430070）

摘 要： 由于传统电极材料低导电性、缓慢的离子扩散速率及较差的稳定性，已无法满足日益增长的能量存储和便携设备需求。石墨烯纳米片组装构建的石墨烯组装膜（Graphene Assembled Films, GAFs）展现出超高的导电性、独特的二维结构与卓越的力学稳定性等综合优势，为解决上述问题提供潜力。然而，目前对于 GAFs 作为先进电极材料的系统认知仍显不足。本综述聚焦 GAFs 在电化学领域的应用，通过全面解析其合成方法、表面/结构特征和物理性质，揭示其结构-性能关系。系统评估其在电池、超级电容器和电化学传感器中的优势，重点论证其优异的电荷传导能力、离子传输动力学和界面稳定性。针对现有器件中存在的化学惰性和脆性等问题，提出缺陷工程和杂化结构等解决方案。本文旨在深化 GAFs 在电化学系统中的机理认知，并为开发稳定、高性能电极材料提供可实施策略。

关键词： 石墨烯组装膜；电池；超级电容器；电化学传感器；合成方法

中图分类号： TQ127.1+1 **文献标识码：** A

基金项目： 国家自然科学基金面上项目（22279097）；湖北省重点研发计划（技术创新类项目，2023BAB103）；海南省教育厅三亚崖州湾科技城博士研究生科研创新基金联合项目（HSPHDSRF-2024-03-022）.

通讯作者： 刘 波，博士. E-mail: liubo2024@whut.edu.cn；
何大平，教授. E-mail: hedaping@whut.edu.cn

第一作者： †朱永芳和†吉晓东为共同第一作者.

本文的电子版全文由 Elsevier 出版社在 ScienceDirect 上出版（https://www.sciencedirect.com/journal/new-carbon-materials/）